Current Biology, Vol. 15, 2007–2012, November 22, 2005, ©2005 Elsevier Ltd All rights reserved. DOI 10.1016/j.cub.2005.09.051

A Role for Mammalian Diaphanous-Related Formins in Complement Receptor (CR3)-Mediated Phagocytosis in Macrophages

Emma Colucci-Guyon,[1,3,4] Florence Niedergang,[1,3,5] Bradley J. Wallar,[2,6] Jun Peng,[2] Arthur S. Alberts,[2] and Philippe Chavrier[1,*]

[1] Membrane and Cytoskeleton Dynamics Group
Unité mixte de recherche 144
Centre National de la Recherche Scientifique/
Institut Curie
75248 Paris
France

[2] Laboratory of Cell Structure and Signal Integration
Van Andel Research Institute
Grand Rapids, Michigan 49503

Summary

Macrophages, dendritic cells, and neutrophils use phagocytosis to capture and clear off invading pathogens. The process is triggered by the interaction of ligands on the pathogens' surface with specific phagocytic receptors, including immunoglobulin (FcR) and complement C3bi (CR3) receptors (integrin $\alpha_M\beta_2$, Mac1) [1]. Localized actin-filament assembly that acts as the driving force for particle engulfment is controlled by Rho-family small GTPases [2, 3]. RhoA regulates CR3-mediated phagocytosis through a mechanism that is still unclear [4–6]. Mammalian Diaphanous-related (mDia) formins participate in the generation of a diverse set of actin-remodeling events downstream of RhoA [7], and mDia1 is recruited around fibronectin-coated beads in a RhoA-dependent manner in fibroblasts [8]. Here, we set out to examine whether mDia proteins are involved in CR3-mediated phagocytosis in macrophages. We show that the RhoA effector mDia1 is recruited early during CR3-mediated phagocytosis and colocalizes with polymerized actin in the phagocytic cup. Interfering with mDia activity inhibits CR3-mediated phagocytosis while having no effect on FcR-mediated phagocytosis. These results indicate a new function for mDia proteins in the regulation of actin polymerization during CR3-mediated phagocytosis.

Results and Discussion

mDia Proteins Are Required for CR3-Mediated, but Not FcR-Mediated, Phagocytosis

Formins are evolutionarily conserved proteins that contain conserved formin homology-1 (FH1) and -2 (FH2) domains [7, 9, 10]. The FH2 domain is necessary and sufficient to nucleate and elongate actin filaments at the barbed end by a novel mechanism that differs from the branched network initiated by the Arp2/3 complex [11–14]. In addition to the FH1 and FH2 domains, the mammalian Diaphanous-related formins mDia1, mDia2, and mDia3 have additional conserved modules: an amino-terminal Rho GTPase binding domain (GBD) and a Diaphanous-autoinhibitory domain (DID) that binds to the carboxy-terminal Diaphanous autoregulatory domain (DAD) as part of an autoregulatory mechanism [7, 15–18]. mDia proteins are thought to be activated by GTPase's binding to the GBD, which disrupts—probably through an allosteric mechanism—the interaction of DID with DAD [11, 17, 19, 20].

Expression of mDia formins mDia1 and mDia2 was detected in RAW264.7 macrophages and in bone-marrow-derived mouse macrophages (Figure 1A). We analyzed by immunofluorescence the distribution of mDia1 during CR3-mediated phagocytosis. Ten minutes after contact of RAW264.7 macrophages with C3bi-opsonized sheep red blood cells (C3bi-SRBCs), the recruitment of endogenous mDia1 was clearly visible in 76.5% ± 1.5% (169 F-actin cups examined from three independent experiments) of the phagocytic cups labeled with F-actin (Figure 1B).

The role of mDia1 and mDia2 during FcR- and CR3-mediated phagocytosis was first addressed by the expression of several mDia2-derived constructs (Figure 1C) known to interfere with the function of endogenous mDia proteins in RAW264.7 cells [21, 22]. As reported previously [4, 23, 24], the expression of dominant inhibitory alleles of Cdc42 ($Cdc42^{T17N}$) or of RhoA ($RhoA^{T19N}$) led to 80% inhibition of FcR- and CR3-mediated phagocytosis, respectively (Figures 1D and 1E, hatched bars). None of the mDia-interfering constructs affected FcR-mediated phagocytosis (Figure 1D). In contrast, expression of ΔGBDΔDAD−G(YEKR)-mDia2 (see Figure 1C) [22, 25] and ΔGBDΔFH1-mDia2 [21] reduced the efficiency of CR3-mediated phagocytosis by 55% and 80%, respectively (Figure 1E). The isolated GTPase binding domain of mDia2 (GBD-mDia2), which binds to GTP-RhoA and probably competes with endogenous downstream effectors, led to 80% inhibition of uptake (Figure 1E). Importantly, none of these constructs significantly affected the binding of particles to the macrophages (Figures 1D and 1E, black bars).

We further addressed the role of mDia in CR3-mediated phagocytosis by using the siRNA approach to knockdown its expression in RAW264.7 cells. Despite several attempts with three different RNA sequences, reducing the level of mDia2 was unsuccessful. In contrast, two independent siRNAs directed against mDia1 led to a substantial decrease in its expression (Figure 2A). The efficiency of particle binding and uptake was monitored in mDia1-depleted cells identified by immunostaining with anti-mDia1 antibodies. Although association was not affected in mDia1-depleted cells, particle internalization was reduced by 50% (Figure 2B). The inhibition of phagocytosis in mDia1-depleted cells was

*Correspondence: philippe.chavrier@curie.fr
[3] These authors contributed equally to this work.
[4] Present address: Macrophages and Development of Immunity Group, unité de recherche associée 2578, Centre National de la Recherche Scientifique, Institut Pasteur, 75015 Paris, France.
[5] Present address: Institut Cochin, unité mixte de recherche 8104, Centre National de la Recherche Scientifique, U567 Institut de la Santé et de la Recherche Médicale, 75014 Paris, France.
[6] Present address: Chemistry Department, Grand Valley State University, 368 Padnos Hall, Allendale, Michigan 49401-9403.

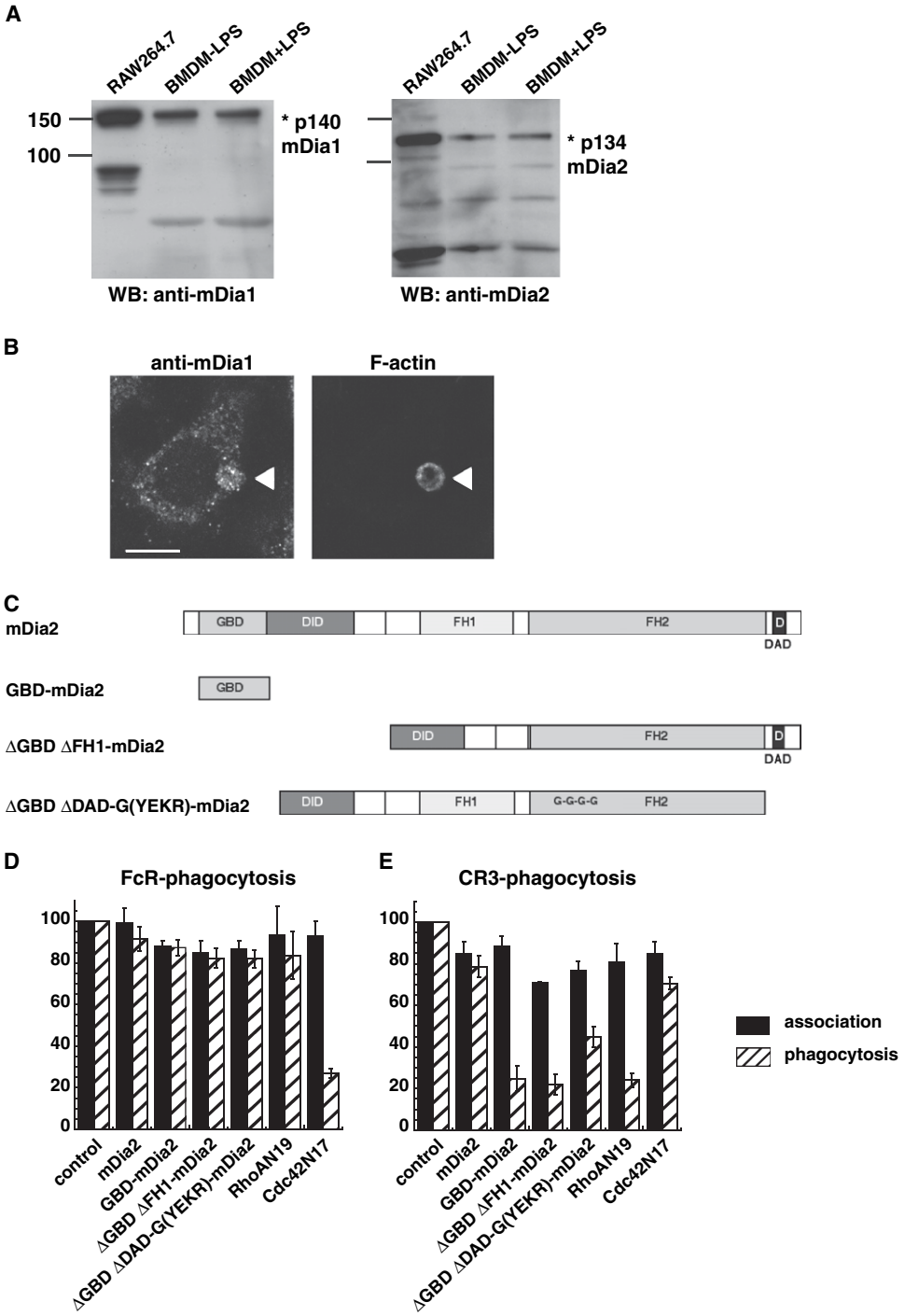

Figure 1. mDia1 and mDia2 Are Expressed in Macrophages, Colocalize with F-Actin in the Phagocytic Cup, and Are Specifically Required for Efficient CR3-Mediated Phagocytosis

(A) mDia1 and mDia2 are constitutively expressed in both RAW264.7 cells and in bone marrow-derived macrophages (BMDM). Cell lysates from RAW264.7 macrophages and from resting (BMDM-LPS) or activated (BMDM+LPS) bone marrow-derived mouse macrophages were analyzed by Western blotting with specific mDia1 (left panel) and mDia2 (right panel) antibodies.

(B) RAW264.7 cells were incubated at 37°C with C3bi-SRBCs for 10 min. The cells were then fixed, and external C3bi-SRBCs were detected with Cy2-anti-rabbit IgG (arrowheads) before permeabilization and staining with mDia1 antibodies followed by Cy3-anti-mouse IgG (left panel) and Alexa350-phalloidin (right panel). Labeled cells were analyzed by wide-field microscopy with deconvolution (one medial section is shown). Endogenous mDia1 was recruited at the site of particle ingestion and colocalized with F-actin in 76.5% of the phagocytic cups (n = 169 phagocytic cups scored). The scale bar represents 10 μm.

(C) Schematic representation of the GFP-mDia2-derived constructs used for interfering with mDia activity. GGGG indicates the site of G(YEKR) mutation generated the substitution of Gly for Tyr-713, Glu-714, Lys-715, and Arg-717, with Ile 716 left intact [25].

(D) mDia2-derived constructs have no effect on FcR-mediated phagocytosis. RAW264.7 macrophages transiently expressing the mDia2-derived constructs or the dominant-negative mutants $RhoA^{T19N}$ and $Cdc42^{T17N}$ were allowed to phagocytose IgG-SRBCs for 60 min at 37°C. The cells

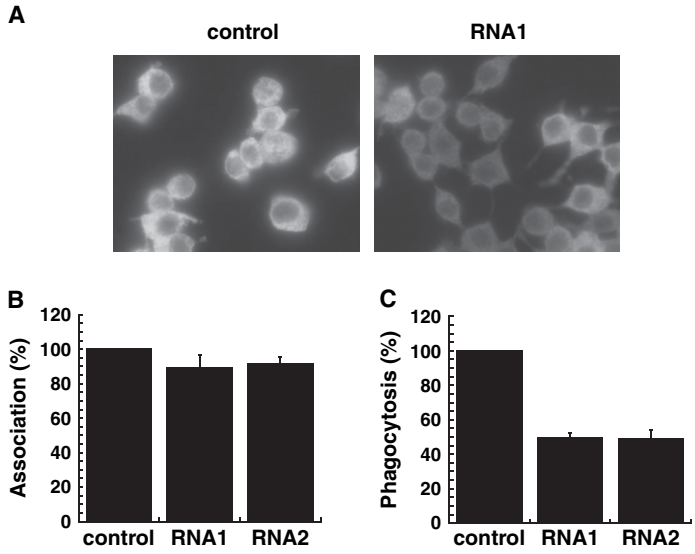

Figure 2. mDia1 siRNA Treatment Inhibits CR3-Mediated Phagocytosis

(A) RAW264.7 macrophages were transfected with siRNA directed against mDia1 or irrelevant siRNA used as a control. After 24 hr, the cells were fixed, permeabilized, and then stained with anti-mDia1 antibodies followed by Cy3-anti-mouse IgG and observed by wide-field fluorescence microscopy. The mDia1-depleted cells showed a decreased mDia1-positive fluorescent signal compared with the bright non-depleted cells and were detectable under the microscope (results with RNA.1 are shown).

(B) Transfected cells were allowed to phagocytose C3bi-SRBCs for 60 min at 37°C. The cells were then fixed, and external C3bi-SRBCs were detected with Cy2-anti-rabbit IgG before permeabilization and staining with anti-mDia1 antibodies followed by Cy3-anti-mouse IgG and Alexa350-phalloidin. The efficiency of association was calculated on 50 mDia1-depleted and 50 control cells transfected with an irrelevant siRNA. Results are expressed as a percentage of control cells. Means ± S.E.M. of three independent experiments are plotted.

(C) Cells were treated as described in (B), and the efficiency of phagocytosis was calculated on 50 mDia1-depleted and 50 control cells transfected with an irrelevant siRNA. Results are expressed as a percentage of control cells. Means ± S.E.M. of three independent experiments are plotted.

not as strong as that observed in cells expressing mDia2-derived constructs (compare Figures 1E and 2C), possibly because the latter were able to interfere with the activity of both mDia1 and mDia2 proteins. Together, these results indicate that mDia1, mDia2, or both are critical for CR3-mediated phagocytosis in macrophages.

mDia Controls Actin Assembly during CR3-Mediated Phagocytosis

Inhibition of the RhoA downstream effector ROCK either with the ROCK inhibitor Y-27632 or with a dominant inhibitory kinase-dead ROCK-domain construct inhibits CR3-mediated phagocytosis, indicating that ROCK plays an important role in this process [6]. We therefore tested whether mDia and ROCK could cooperate during phagocytosis. Simultaneous inhibition of mDia1 (by RNAi) and ROCK (dominant inhibitory kinase-dead domain [26]) led to a 64% ± 2.8% inhibition of CR3-mediated phagocytosis. This effect was significantly stronger than what was observed after blocking the mDia and ROCK activities separately (51% ± 3.8% and 43% ± 3.8%, respectively) (Figure 3C), suggesting that the two RhoA effectors contribute to CR3-mediated phagocytosis.

Because mDia1 has been shown to control actin polymerisation downstream of RhoA [8, 27], we then assessed whether interfering with mDia activity had any effect on actin assembly during CR3-mediated phagocytosis. As reported [5], actin accumulation was inhibited in cells transiently expressing $RhoA^{T19N}$, whereas it was similar to controls in cells expressing $Cdc42^{T17N}$ (Figure 4A). The expression of mDia2-derived constructs and knockdown of mDia1 similarly decreased F-actin recruitment around the particles (Figures 4A and 4B), showing that mDia1 and mDia2 contribute to actin polymerization during CR3-mediated phagocytosis.

To further characterize cells depleted for mDia1, we performed scanning electron microscopy analysis after 60 min of phagocytosis. Although most of the particles were internalized in control cells (Figure 4C, left panel), many remained at the surface of depleted cells with no sign of engulfment (Figure 4C, right panel). These results indicate that mDia1 controls an early step during CR3-mediated phagocytosis.

In summary, our results demonstrate for the first time that mDia formins play a critical role in CR3-mediated phagocytosis. The dual engagement of both mDia (our data) and the Arp2/3 complex [6] during CR3-mediated phagocytosis, in contrast to FcR-mediated phagocytosis, which does not require mDia activity, provides a new molecular basis for explaining differences in the early events of IgG- or complement-opsonized particle engulfment [4, 28, 29].

Experimental Procedures

Plasmids and Reagents

pEGFP-mDia2 (JP002) encodes full-length mDia2 (GenBank Accession AF094519) fused to EGFP. GBD-mDia2, ΔGBDΔFH1-mDia2, and ΔGBDΔDAD-G(YEKR)-mDia2 fused to EGFP were described previously [16, 21, 22, 25]. We generated the G(YEKR) mutation by

were then fixed, and external SRBCs were stained with Cy3-anti-rabbit IgG antibodies. The efficiencies of association (black bars) and phagocytosis (hatched bars) were scored in 50 transfected and 50 control cells (GFP-negative transfected cells). Results are expressed as a percentage of control cells. The means ± S.E.M. of three independent experiments are plotted.

(E) mDia2-derived constructs inhibited CR3-mediated phagocytosis. RAW264.7 macrophages transiently expressing mDia2-derived constructs or the dominant-negative mutants $RhoA^{T19N}$ and $Cdc42^{T17N}$ were incubated with 150 ng/ml PMA to activate CR3, were then allowed to phagocytose C3bi-SRBCs for 60 min at 37°C, and were processed as in (D). The means ± S.E.M. of three independent experiments are plotted. Control, GFP-negative transfected cells.

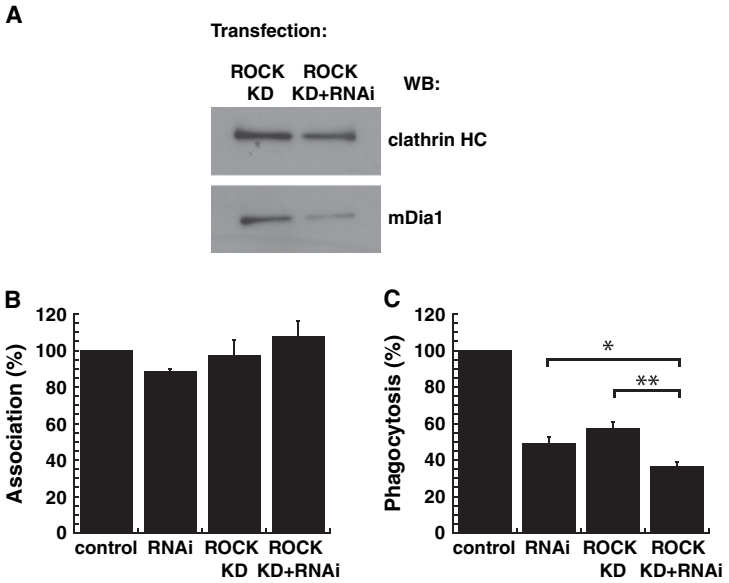

Figure 3. Effect of Simultaneous Inhibition of mDia and ROCK during CR3-Mediated Phagocytosis

(A) Lysates from RAW264.7 cells expressing ROCK-KD or those expressing ROCK-KD and also depleted for mDia1 were analyzed by Western blotting with mDia1 antibody (lower panel) and clathrin HC antibody (upper panel).

(B) RAW264.7 cells transiently transfected with an irrelevant siRNA (control), siRNA against mDia1 (RNAi), pRK5-myc-ROCK-KD plasmid (ROCK-KD), or both mDia1 siRNA and pRK5-Myc-ROCK-KD (ROCK-KD+RNAi) were incubated with C3bi-SRBCs for 60 min at 37ºC. After fixation and staining of external C3bi-SRBCs with Cy2-anti-rabbit IgG, cells were permeabilized and labeled with Dia1 or Myc antibodies followed by Cy3-anti-mouse IgG. We checked in an independent experiment that cells cotransfected with Myc-ROCK-KD plasmid and mDia1 siRNA showed a diminished expression of mDia1 (not shown). Fifty transfected and/or depleted cells and 50 control cells were scored for association efficency. Results are expressed as a percentage of control cells. The means ± S.E.M. of three independent experiments are plotted.

(C) Cells were treated as described in (B), and the efficiency of phagocytosis was calculated on 50 mDia1-depleted and 50 control cells. Results are expressed as a percentage of control cells. Means ± S.E.M. of four independent experiments are plotted. The statistical significance of these data was tested with an unpaired Student's t test with a goodness-of-fit value of $p < 0.05$ (*) or $p < 0.005$ (**).

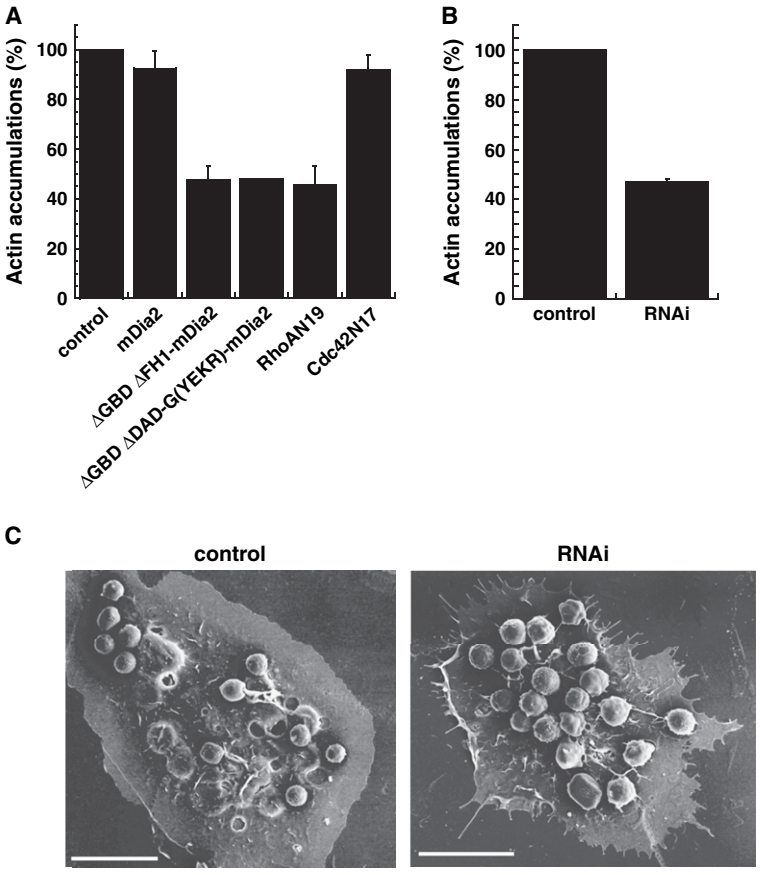

Figure 4. Inhibition of mDia Activity Results in Decreased F-Actin Recruitment and Early Blockade of Phagocytosis

(A) RAW264.7 macrophages transiently expressing GFP-tagged-mDia2-derived constructs or dominant-negative mutants $RhoA^{T19N}$ and $Cdc42^{T17N}$ were incubated with C3bi-SRBCs at 37ºC for 5 min. Cells were fixed and stained with Cy3-anti-rabbit IgG to detect the external particles. F-actin was labeled with Alexa350-phalloidin. Fifty GFP-positive cells and 50 GFP-negative control cells were scored for the presence or absence of F-actin accumulation around bound particles as described in the Experimental Procedures section. Results are expressed as a percentage of control cells. Means ± S.E.M. of three independent experiments are plotted except those for ΔGBDΔDAD-G(YEKR)-mDia2-expressing cells (two experiments are plotted).

(B) RAW264.7 cells were treated with siRNA against mDia1 or with an irrelevant siRNA (control) and incubated with C3bi-SRBCs for 5 min at 37ºC. Cells were fixed, and external particles were labeled with Cy5-anti-rabbit IgG. F-actin was stained with Alexa350-phalloidin. mDia1 siRNA-treated cells (50) and control cells (50) were scored for F-actin accumulation as described in the legend of panel 4A. The means ± S.E.M. of three independent experiments are plotted.

(C) RAW264.7 macrophages were cotransfected with pEGFP-N1 plasmid and siRNA specific for mDia1 or an irrelevant siRNA (control). We verified on a separate coverslip by immunofluorescence staining with anti-mDia1 antibody that GFP-positive, siRNA mDia1-treated cells were indeed depleted for mDia1 (not shown). Transfected cells were grown on CeLLocate coverslips, incubated with C3bi-SRBCs for 60 min at 37ºC, and fixed. GFP-positive cells were located on coverslips by fluorescence microscopy and were analyzed by scanning electron microscopy. The scale bars represent 10 μm.

substituting Gly for Tyr-713, Glu-714, Lys-715, and Arg-717 and leaving Ile-716 intact [25]. The pEGFPL11-Cdc42^{T17N} and pEGFP-RhoA^{T19N} plasmids were kind gifts from Dr. P. Fort (UPR 1086, Montpellier, France). The pRK5-Myc-ROCK-KD vector [6, 26], encoding the ROCK catalytic domain mutated in the ATP binding site (lacking the Rho binding domain) was kindly provided by Dr. L. Machesky (University of Birmigham, UK). The pEGFP-N1 plasmid was from Clontech.

PMA (phorbol 12-myristate 13-acetate) was from Sigma. The following antibodies were used: anti-mDia1 (BD Transduction Laboratory);anti-mDia2 (C-15, Santa Cruz Biotechnology); anti-Myc (Roche); anti-clathrin heavy chain (Becton Dickinson); Cy2-, Cy3-, or Cy5-labeled F(ab′)2 anti-mouse and anti-rabbit IgG (Jackson Immunoresearch); HRP-labeled anti-mouse IgG (Sigma); and HRP-labeled anti-goat IgG (Jackson Immunoresearch). Alexa350-coupled phalloidin was from Molecular Probes.

Cell Culture, Transfection, and siRNA Treatment

RAW264.7 macrophages were grown and transfected as described [30]. Bone-marrow-derived macrophages were cultivated from 7-week-old mouse femoral and tibial bones as described [31].

RAW264.7 macrophages were transfected with siRNA duplex (Proligo) specific for mouse Dia1 or for GFP with Lipofectamine 2000 according to the manufacturer's instructions (Invitrogen [32]). The mDia1-specific siRNA sequences were (RNA.1) 5′-AGCCAG GCCACAGUACUAU-3′ and (RNA.2) 5′-GCUGGUCAGAGCCAUGG AU-3′, as described [33]. The SiRNA duplex against GFP used as a negative control was described [34]. After 24 and 48 hr, cell lysates were analyzed by Western blotting as described [34]. When indicated, siRNA and expression plasmids were cotransfected in the cells. In those cases we verified by immunofluorescence with an mDia1 antibody that cells transiently expressing the indicated construct were depleted for mDia1.

Phagocytosis Assays

Phagocytosis was performed as described [30, 34]. To quantitate phagocytosis, we counted the number of internalized SRBCs in 50 randomly chosen cells on the coverslips and calculated the phagocytic index, i.e., the mean number of phagocytosed SRBCs per cell. The index obtained for transfected cells was divided by the index obtained for control transfected non-expressing cells and expressed as a percentage of control cells. We also counted the number of cell-associated (bound + internalized) SRBCs, calculated the association index (mean number of associated SRBCs per cell), and expressed it as percentage of control cells. To quantitate polymerized actin recruitment, we scored the presence or absence of F-actin accumulations around particles in 50 randomly chosen cells on the coverslips and calculated an accumulation index, i.e., the mean number of accumulations per cell. The index obtained for the siRNA mDia1-treated cells was divided by the index obtained for control (siRNA GFP) cells and expressed as a percentage of the latter.

Immunofluorescence Analysis

Cells were fixed in 4% paraformaldehyde/phosphate-buffered saline and labeled [30]. Cells were examined under a motorized upright wide-field microscope (Leica DMRA2) equipped for image deconvolution. Acquisition was performed with an oil-immersion objective lens (100× PL APO HCX, 1.4 NA) and a cooled CCD camera (Roper CoolSnap HQ). Z positioning was accomplished by a piezo-electric motor, and deconvolution was performed as described [34]. Acquisitions were also performed with a motorized upright wide-field microscope (Leica DM RXA2) equipped with an oil-immersion objective lens (63× PL APO HCX, 1.32 NA) and a cooled CCD camera (Roper CoolSnap HQ).

Scanning Electron Microscopy Analysis

Macrophages were prepared for scanning electron microscopy as described [31], except that transiently transfected RAW264.7 cells were plated onto CeLLocate (Eppendorf) coverslips to allow the localization of siRNA-treated cells coexpressing GFP under a fluorescence microscope and the observation of the same cells by scanning electron microscopy.

Acknowledgments

We thank Franco Ardizzoni (Centre de Microscopie Electronique, Lausanne) for help with the scanning electron microscope, Vincent Fraisier and Jean-Baptiste Sibarita (unité mixte de recherche 144, Institut Curie) for image deconvolution, and Jean-François Alkombre (Institut National de la Recherche Agronomique, Centre de Jouy-en-Josas) for collecting blood samples. This work was supported by grants from the Centre National de la Recherche Scientifique, Institut Curie, Fondation BNP-Paribas and La Ligue Nationale contre le Cancer ("équipe labellisée") to P.C. and from the Fondation pour la Recherche Médicale (INE20041102865) to F.N.. The Congressionally Directed Medical Breast Cancer Research Program (DAMD17-00-1-0190) and The Van Andel Foundation supported A.S.A.; additional support to A.S.A. and J.P. was provided by the National Cancer Institute (R21 CA107529) and the American Cancer Society (RSG-05-033-01-CSM). We are grateful to Dr. Francesco Colucci for critical reading of the manuscript and to David Nadziejka (Van Andel Research Institute) for scientific editing.

Received: July 20, 2005
Revised: September 7, 2005
Accepted: September 26, 2005
Published: November 21, 2005

References

1. Aderem, A., and Underhill, D.M. (1999). Mechanisms of phagocytosis in macrophages. Annu. Rev. Immunol. *17*, 593–623.
2. Greenberg, S., and Grinstein, S. (2002). Phagocytosis and innate immunity. Curr. Opin. Immunol. *14*, 136–145.
3. Niedergang, F., and Chavrier, P. (2004). Signaling and membrane dynamics during phagocytosis: Many roads lead to the phagos(R)ome. Curr. Opin. Cell Biol. *16*, 422–428.
4. Caron, E., and Hall, A. (1998). Identification of two distinct mechanisms of phagocytosis controlled by different rho GTPases. Science *282*, 1717–1721.
5. May, R.C., Caron, E., Hall, A., and Machesky, L.M. (2000). Involvement of the Arp2/3 complex in phagocytosis mediated by FcgR or CR3. Nat. Cell Biol. *2*, 246–248.
6. Olazabal, I.M., Caron, E., May, R.C., Schilling, K., Knecht, D.A., and Machesky, L.M. (2002). Rho-kinase and myosin-II control phagocytic cup formation during CR, but not FcgammaR, phagocytosis. Curr. Biol. *12*, 1413–1418.
7. Wallar, B.J., and Alberts, A.S. (2003). The formins: Active scaffolds that remodel the cytoskeleton. Trends Cell Biol. *13*, 435–446.
8. Watanabe, N., Madaule, P., Reid, T., Ishizaki, T., Watanabe, G., Kakizuka, A., Saito, Y., Nakao, K., Jockusch, B.M., and Narumiya, S. (1997). p140mDia, a mammalian homolog of Drosophila diaphanous, is a target protein for Rho small GTPase and is a ligand for profilin. EMBO J. *16*, 3044–3056.
9. Castrillon, D.H., and Wasserman, S.A. (1994). Diaphanous is required for cytokinesis in Drosophila and shares domains of similarity with the products of the limb deformity gene. Development *120*, 3367–3377.
10. Higgs, H.N., and Peterson, K.J. (2005). Phylogenetic analysis of the formin homology 2 domain. Mol. Biol. Cell *16*, 1–13.
11. Pruyne, D., Evangelista, M., Yang, C., Bi, E., Zigmond, S., Bretscher, A., and Boone, C. (2002). Role of formins in actin assembly: nucleation and barbed-end association. Science *297*, 612–615.
12. Sagot, I., Rodal, A.A., Moseley, J., Goode, B.L., and Pellman, D. (2002). An actin nucleation mechanism mediated by Bni1 and profilin. Nat. Cell Biol. *4*, 626–631.
13. Zigmond, S.H. (2004). Formin-induced nucleation of actin filaments. Curr. Opin. Cell Biol. *16*, 99–105.
14. Otomo, T., Tomchick, D.R., Otomo, C., Panchal, S.C., Machius, M., and Rosen, M.K. (2005). Structural basis of actin filament nucleation and processive capping by a formin homology 2 domain. Nature *433*, 488–494.
15. Watanabe, N., Kato, T., Fujita, A., Ishizaki, T., and Narumiya, S. (1999). Cooperation between mDia1 and ROCK in Rho-induced actin reorganization. Nat. Cell Biol. *1*, 136–143.

16. Alberts, A.S. (2001). Identification of a carboxyl-terminal diaphanous-related formin homology protein autoregulatory domain. J. Biol. Chem. *276*, 2824–2830.
17. Li, F., and Higgs, H.N. (2003). The mouse Formin mDia1 is a potent actin nucleation factor regulated by autoinhibition. Curr. Biol. *13*, 1335–1340.
18. Li, F., and Higgs, H.N. (2005). Dissecting requirements for autoinhibition of actin nucleation by the formin, mDia1. J. Biol. Chem. *280*, 6986–6992.
19. Zigmond, S.H., Evangelista, M., Boone, C., Yang, C., Dar, A.C., Sicheri, F., Forkey, J., and Pring, M. (2003). Formin leaky cap allows elongation in the presence of tight capping proteins. Curr. Biol. *13*, 1820–1823.
20. Evangelista, M., Zigmond, S., and Boone, C. (2003). Formins: Signaling effectors for assembly and polarization of actin filaments. J. Cell Sci. *116*, 2603–2611.
21. Tominaga, T., Sahai, E., Chardin, P., McCormick, F., Courtneidge, S.A., and Alberts, A.S. (2000). Diaphanous-related formins bridge Rho GTPase and Src tyrosine kinase signaling. Mol. Cell *5*, 13–25.
22. Peng, J., Wallar, B.J., Flanders, A., Swiatek, P.J., and Alberts, A.S. (2003). Disruption of the Diaphanous-related formin Drf1 gene encoding mDia1 reveals a role for Drf3 as an effector for Cdc42. Curr. Biol. *13*, 534–545.
23. Cox, D., Chang, P., Zhang, Q., Reddy, P.G., Bokoch, G.M., and Greenberg, S. (1997). Requirements for both rac1 and cdc42 in membrane ruffling and phagocytosis in leukocytes. J. Exp. Med. *186*, 1487–1494.
24. Massol, P., Montcourrier, P., Guillemot, J.C., and Chavrier, P. (1998). Fc receptor-mediated phagocytosis requires CDC42 and Rac1. EMBO J. *17*, 6219–6229.
25. Wen, Y., Eng, C.H., Schmoranzer, J., Cabrera-Poch, N., Morris, E.J., Chen, M., Wallar, B.J., Alberts, A.S., and Gundersen, G.G. (2004). EB1 and APC bind to mDia to stabilize microtubules downstream of Rho and promote cell migration. Nat. Cell Biol. *6*, 820–830.
26. Amano, M., Chihara, K., Kimura, K., Fukata, Y., Nakamura, N., Matsuura, Y., and Kaibuchi, K. (1997). Formation of actin stress fibers and focal adhesions enhanced by Rho-kinase. Science *275*, 1308–1311.
27. Higashida, C., Miyoshi, T., Fujita, A., Oceguera-Yanez, F., Monypenny, J., Andou, Y., Narumiya, S., and Watanabe, N. (2004). Actin polymerization-driven molecular movement of mDia1 in living cells. Science *303*, 2007–2010.
28. Kaplan, G. (1977). Differences in the mode of phagocytosis with Fc and C3 receptors in macrophages. Scand. J. Immunol. *6*, 797–807.
29. Allen, L.A., and Aderem, A. (1996). Molecular definition of distinct cytoskeletal structures involved in complement- and Fc receptor-mediated phagocytosis in macrophages. J. Exp. Med. *184*, 627–637.
30. Niedergang, F., Colucci-Guyon, E., Dubois, T., Raposo, G., and Chavrier, P. (2003). ADP ribosylation factor 6 is activated and controls membrane delivery during phagocytosis in macrophages. J. Cell Biol. *161*, 1143–1150.
31. Niedergang, F., Sirard, J.C., Blanc, C.T., and Kraehenbuhl, J.P. (2000). Entry and survival of Salmonella typhimurium in dendritic cells and presentation of recombinant antigens do not require macrophage-specific virulence factors. Proc. Natl. Acad. Sci. USA *97*, 14650–14655.
32. Elbashir, S.M., Lendeckel, W., and Tuschl, T. (2001). RNA interference is mediated by 21- and 22-nucleotide RNAs. Genes Dev. *15*, 188–200.
33. Arakawa, Y., Bito, H., Furuyashiki, T., Tsuji, T., Takemoto-Kimura, S., Kimura, K., Nozaki, K., Hashimoto, N., and Narumiya, S. (2003). Control of axon elongation via an SDF-1alpha/Rho/mDia pathway in cultured cerebellar granule neurons. J. Cell Biol. *161*, 381–391.
34. Braun, V., Fraisier, V., Raposo, G., Hurbain, I., Sibarita, J.B., Chavrier, P., Galli, T., and Niedergang, F. (2004). TI-VAMP/VAMP7 is required for optimal phagocytosis of opsonised particles in macrophages. EMBO J. *23*, 4166–4176.